FINAL REPORT

Non-chromate Passivation for LHE ZnNi

SERDP Project WP-2527

JANUARY 2017

Matt O'Keefe
Missouri S&T

SERDP
DOD ▪ EPA ▪ DOE

Page Intentionally Left Blank

Page Intentionally Left Blank

REPORT DOCUMENTATION PAGE

Form Approved
OMB No. 0704-0188

1. REPORT DATE *(DD-MM-YYYY)*	2. REPORT TYPE	3. DATES COVERED *(From - To)*
01/03/2017	Final Report	October 2015 - January 2017

4. TITLE AND SUBTITLE
Non-chromate Passivation for LHE ZnNi

5a. CONTRACT NUMBER
W912HQ-15-C-0065

5b. GRANT NUMBER

5c. PROGRAM ELEMENT NUMBER

6. AUTHOR(S)
Prof. Matt O'Keefe
Missouri University of Science & Technology

5d. PROJECT NUMBER
WP-2527

5e. TASK NUMBER

5f. WORK UNIT NUMBER

7. PERFORMING ORGANIZATION NAME(S) AND ADDRESS(ES)
Missouri University of Science & Technology
401 W. 16th Street
Rolla, MO 65409

8. PERFORMING ORGANIZATION REPORT NUMBER

9. SPONSORING/MONITORING AGENCY NAME(S) AND ADDRESS(ES)
Strategic Environmental Research and Development Program Program Office
4800 Mark Center Drive
Suite 17D03
Alexandria, VA 22350-3605

10. SPONSOR/MONITOR'S ACRONYM(S)
SERDP

11. SPONSOR/MONITOR'S REPORT NUMBER(S)

12. DISTRIBUTION/AVAILABILITY STATEMENT
Approved for public release; distribution is unlimited.

13. SUPPLEMENTARY NOTES
N/A

14. ABSTRACT
Missouri University of Science and Technology (Missouri S&T) collaborated with Dipsol of America (Dipsol) and Boeing Research & Technology (BR&T) to develop and evaluate low contact resistance passivation layers for Department of Defense electrical system components. Specifically, the team examined five different types of passivation layers that were free of hexavalent chromium for low hydrogen embrittlement (LHE) ZnNi coatings. Passivations included a trivalent chromium passivation (TCP or Cr(III)), a Co-Free TCP, and a Modified Co-Free TCP developed at Dipsol as well as two cerium based conversion coatings (CeCCs) developed at Missouri S&T using cerium chloride and cerium nitrate sources.

15. SUBJECT TERMS
Electrical components, low contact resistance passivation layers, hexavalent chromium, trivalent chromium passivation, TCP, low hydrogen embrittlement (LHE) ZnNi coatings.

16. SECURITY CLASSIFICATION OF:			17. LIMITATION OF ABSTRACT	18. NUMBER OF PAGES	19a. NAME OF RESPONSIBLE PERSON
a. REPORT	b. ABSTRACT	c. THIS PAGE			Matthew O'Keefe
Unclassified	Unclassified	UU	UL	37	19b. TELEPHONE NUMBER *(Include area code)* 573-341-6764

Page Intentionally Left Blank

Table of Contents

List of Acronyms 3
List of Figures and Tables 4
Acknowledgments 6
Abstract 7
Objective 8
Background 9
Materials and Methods 13
    Cerium-based Passivation Deposition 13
    Trivalent and Hexavalent Chromium Based Passivation Deposition 14
    Corrosion Resistance. 14
    Electrochemical Analysis 14
    Contact Resistance. 15
Results and Discussion 16
  First Set of Passivation Samples 16
  Second Set of Passivation Samples 20
  Alternative Contact Resistance Methodology 30
Conclusions and Implications for Future Research 34
Literature Citations 35
Appendices 37
  Supporting Data 37
  List of Scientific/Technical Publications 37
    Articles in Peer-reviewed Journals 37
    Technical Reports 37
    Conference or Symposium Scientifically Recognized 37
    Conference or Symposium Abstracts 37
    Text Books or Chapters 37
  Other Supporting Materials 37

List of Acronyms

ZnNi: Zinc Nickel
Mil-DTL: Military Detail Specification
ASTM: American Society for Testing and Materials
LHE: Low Hydrogen Embrittlement
TCP: Trivalent Chromium Passivation
CeCCs : Cerium conversion coatings
Cd: Cadmium
Ni: Nickel
PTFE: Polytetraflouroethylene (known as Teflon)
SAE: Society of Automotive Engineers
AMS: Aerospace Material Specification
Al: Aluminum
Pr: Praseodymium
Ce: Cerium
USAMP: United States Automotive Materials Partnership
Mg: Magnesium
Zn: Zinc
CPDS: Cyclic PotentioDynamic Scans
NaCl: Sodium Chloride
OCP: Open Circuit Potential
EIS: Electrochemical Impedance Spectroscopy
SEM: Scanning Electron Microscopy
CrCC: Chromate conversion coatings
CeCC-Cl: Cerium chloride conversion coatings
CeCC-N: Cerium nitrate conversion coatings
HCl: Hydrochloric acid
EG&G:
FIB: Focused Ion Beam
Pt: Platinum
BYU: Brigham Young University

List of Figures and Tables

Figure 1. CPDS of LHE ZnNi coatings on steel substrates that are: a) bare and b) coated with Dipsol IZ-264 trivalent chromium passivation 10
Figure 2. Bare (NCC) and TCP conversion coated (CC) LHE ZnNi coatings on a steel substrate: a) Nyquist plot, b) Bode impedance and phase angle plots 11
Figure 3. Corrosion current density as a function of time for LHE ZnNi coatings on a steel substrate: a) bare and b) coated with Dipsol IZ-264 trivalent chromium passivation 12
Figure 4. SEM images of LHE ZnNI coatings on a steel substrate after FIB sectioning: a) no passivation; and b) with a Dipsol IZ-264 trivalent chromium passivation 12
Figure 5. Process flow chart for deposition of cerium based passivations on LHE ZnNi 13
Figure 6. Process flow chart for depositions of trivalent and hexavalent chromium passivations on LHE ZnNi 14
Figure 7. Electrical contact resistance testing set-up per MIL-STD-81706 15
Figure 8. Optical images of a) uncoated LHE ZnNi surface and b) TCP coated ZnNi surface.. 16
Figure 9. Scanning electron image of the top surface of uncoated electroplated LHE ZnNi 17
Figure 10. Topological profile plot across an uncoated, electroplated LHE ZnNi surface 17
Figure 11. Cross-sectional image of a ~100 nm thick TCP layer on an electroplated ZnNi coating 18
Figure 12. Contact resistance values of as-deposited LHE ZnNi samples with different passivations 18
Figure 13. Images of LHE ZnNi samples with different passivation layers (CeCC are 1-13) after 500 hours of ASTM B117 salt spray exposure 19
Figure 14. Contact resistance values of LHE ZnNi samples with different passivation layers after 500 hours of ASTM B117 salt spray exposure 20
Figure 15. Contact resistance values of as-deposited LHE ZnNi samples with different passivation layers 21
Figure 16. Bode phase angle plots for as-deposited passivation layers on LHE ZnNi 22
Figure 17. Bode phase angle plots for CeCC passivation layers on LHE ZnNi 23
Figure 18. Bode phase angle plots for TCP and CrCC passivation layers on LHE ZnNi 23
Figure 19. Bode phase angle plots for Co-Free and Co-Free Mod passivation layers on LHE ZnNi 24
Figure 20. Polarization curves for all six as-deposited passivation layers 24
Figure 21. Optical images of CeCC passivated ZnNi samples before (left) and after (right) 1000 hours of ASTM B117 neutral salt spray exposure 25
Figure 22. Optical images of standard IZ-264 TCP and CrCC passivated ZnNi samples before 26(left) and after (right) 1000 hours of ASTM B117 neutral salt spray exposure 26
Figure 23. Optical images of Co-Free TCP and Co-Free Mod passivated ZnNi samples before (left) and after (right) 1000 hours of ASTM B117 neutral salt spray exposure 26
Figure 24. Scanning electron microscope images from the surface of CeCC passivated ZnNi samples after 1000 hours of ASTM B117 neutral salt spray exposure 27
Figure 25. Scanning electron microscope images from the surface of standard TCP and CrCC passivated ZnNi samples after 1000 hours of ASTM B117 neutral salt spray exposure 27

Figure 26. Scanning electron microscope images from the surface of standard Co-Free and Co-Free Mod passivated ZnNi samples after 1000 hours of ASTM B117 neutral salt spray exposure 28
Figure 27. Electrical contact resistance values for the six passivation layers prior to and after ASTM B117 salt spray exposure 28
Figure 28. X-ray diffraction patterns for the six passivation layers after 1000 hours of ASTM B117 salt spray exposure 29
Figure 29. Bode phase angle plots for different passivation layers on LHE ZnNi after 1000 hours of ASTM B117 salt spray exposure 30
Figure 30. Four line microprobe geometry 31
Figure 31. Tangential and Orthogonal measurement configuration 31
Figure 32. Probe lines before use 32
Figure 33. Probe lines after use 32

Acknowledgments

Many people and organizations contributed to this project and report. The majority of the data was collected and analyzed by graduate student Steven Volz and research engineer James Claypool. All of the ZnNi substrates and the majority of the passivated samples were provided by Dr. Tarek Nahlawi and his staff at Dipsol of America. Steve Gaydos at Boeing provided technical guidance and direction throughout the project. Prof. Bill Fahrenholtz served has co-investigator at Missouri S&T. The support of the staff of the Graduate Center for Materials Research Center at Missouri S&T assisted in characterizing the samples and providing administrative support. The efforts of all those involved are gratefully acknowledged.

Abstract

The electrochemical response, corrosion behavior, and electrical contract resistance of cerium based, trivalent chromium based, and hexavalent chromium based passivations on electroplated, low hydrogen embrittlement γ-ZnNi coatings on steel substrates were evaluated.

Deposition processes that resulted in ~100 nm thick passivations with as-deposited contact resistances < 5 mΩ/in^2 as measured by MIL-DTL-81706B were developed for all of the passivations studied. The electrochemical response of the as-deposited passivations on the γ-ZnNi was dependent on the type of passivation. Cerium based passivations demonstrated a simple barrier type of electrochemical impedance with a peak phase angle value near 60°. Standard trivalent chromium and hexavalent chromium samples had a complex electrochemical impedance indicative of non-barrier type of response with a maximum phase angle of ~45°. Cobalt-free and modified cobalt-free trivalent chromium passivations had maximum phase angles between 20° and 30° and impedance curves that were indicative of active protection. Electrochemical polarization measurements of the as-deposited samples showed a difference in the open circuit potential between -1.1V and -0.9V depending on the passivation. However, once the passivation was compromised and corrosion started all of the samples had a measured corrosion potential of -0.67V, consistent with the value for formation of ZnO.

Neutral salt-spray testing per ASTM B117 of passivated γ-ZnNi coatings on steel substrates out to 1000 hours of exposure was conducted. Results from the testing indicated that extensive corrosion product was observed on the cerium based and cobalt free trivalent chromium samples and that the measured electrical resistance increased several orders of magnitude in value. After 1000 hours of testing the hexavalent chromium samples had visible corrosion product and a few orders of magnitude increase in contact resistance. The cobalt free modified samples were found to have had a few areas with visible corrosion product and a contact resistance value less than the maximum allowable value of 10 mΩ/in^2. The standard trivalent chromium passivation had little to no visible corrosion product after 1000 hours of ASTM B117 exposure and contact resistance values at or below the 10 mΩ/in^2 specification. Characterization of corrosion product by scanning electron microscopy and x-ray diffraction analysis indicated that all samples had similar corrosion products consistent with zinc oxide/hydroxide/carbonate structures but the morphology and appearance of the corrosion product was dependent on the type of passivation used.

Collectively the results of the study indicated that the passivation layer on top of the electroplated γ-ZnNi coatings significantly influenced the electrochemical response, corrosion behavior, and electrical contact resistance of the samples. It was found that the standard trivalent chromium and cobalt free modified passivations on electroplated, low hydrogen embrittlement γ-ZnNi coatings on steel substrates were able to achieve a contact resistance of < 10 mΩ/in^2 after 1000 hours of ASTM B117 salt spray exposure.

Objective

Missouri University of Science and Technology (Missouri S&T) collaborated with Dipsol of America (Dipsol) and Boeing Research & Technology (BR&T) to develop and evaluate low contact resistance passivation layers for Department of Defense electrical system components. Specifically, the team examined five different types of passivation layers that were free of hexavalent chromium for low hydrogen embrittlement (LHE) ZnNi coatings. Passivations included a trivalent chromium passivation (TCP or Cr(III)), a Co-Free TCP, and a Modified Co-Free TCP developed at Dipsol as well as two cerium based conversion coatings (CeCCs) developed at Missouri S&T using cerium chloride and cerium nitrate sources. Hexavalent chromium passivation on electroplated ZnNi was used as a reference. Characterization of the electrical, electrochemical, corrosion, and materials performance of the passivation layers was done to evaluate the corrosion performance and electrical resistance after neutral salt spray exposure. The major outcome of this project was to identify the most promising passivation layer(s) that are free of hexavalent chromium and can be used on LHE ZnNi plated electrical connectors for military electrical system components.

Background

Electroplated Cd has been used for decades as a surface finish on metallic substrates due to desirable properties such as galvanic compatibility with commonly used materials, a non-reflective appearance, excellent corrosion protection, and low electrical resistance [1]. Unfortunately, Cd and Cd plating operations have many undesirable attributes, especially those related to effluents, toxicity, and carcinogenic nature of the materials that lead to stringent restrictions and regulations [2]. Replacement of Cd plated coatings with electroplated low hydrogen embrittlement (LHE) ZnNi has been shown to be effective when the ZnNi is passivated with a conversion coating [3,4,5]. Chromate conversion coatings applied to electroplated ZnNi improve corrosion resistance. Unfortunately, chromate conversion coatings also result in the use of, and exposure to, toxic and carcinogenic hexavalent chromium compounds [6]. A variety of corrosion inhibitors have been developed as environmentally friendly alternatives to chromates for a range of applications [3-8]. Environmentally friendly coatings have the potential to enhance military readiness and reduce costs by providing the necessary corrosion protection and electrical performance without the environmental and health risks associated with chromates.

Several alternatives to Cd plated surface finishes have been investigated, each of which has positive attributes and deficiencies [9]. Three alternate connector finishes are available to replace Cd on military/aerospace applications: Ni-fluorocarbon PTFE (SAE AMS-2454), ZnNi (ASTM B841, AMS 2417), and pure Al (Mil-DTL-83488) [10]. All three are electrically conductive; however, the ZnNi and Al coatings require a chromate treatment to meet both electrical and corrosion inhibition requirements. Over the past 20 years, Missouri S&T and Boeing have collaborated on research and development projects to develop alternatives to coatings containing hexavalent chromium. Initially this work examined a number of different materials, including conducting polymers and rare-earth compounds [11]. After assessing the overall technical and economic life cycle impacts, praseodymium (Pr) and cerium (Ce) based rare-earth compounds were identified as the most promising replacements for chromates in primers (Pr) and conversion coatings on high strength aluminum alloy substrates [12,13]. This work led to development, licensing, and military qualification and approval of a Pr-based inhibitor technology by Deft, Inc (now PPG Aerospace). The family of Pr-based primers is currently being used a number of military aircraft, including the F-15 and F-35 fighters as well as Apache helicopters. Likewise, cerium-based conversion coatings (CeCCs) are effective replacements for chromate conversion coatings. As part of a previous SERDP project, CeCCs were shown to be effective conversion coatings when used in combination with UV curable primers on high strength Al alloys used for aerospace applications [14]. In addition, the corrosion protection mechanisms of CeCCs and primers containing Pr-based corrosion inhibitors were also examined as part of a second SERDP project [15]. Recent work sponsored by the Department of Energy through the U.S. Automotive Materials Program (USAMP) has demonstrated that the CeCCs can be simultaneously deposited on substrates produced by joining an Mg alloy, an Al alloy, and Zn coated steel [16].

WPSEED-15-02 was focused on low contact resistance passivation layers that are compatible with LHE ZnNi used for electrical components. Unpublished research conducted at Missouri S&T for Boeing showed the importance of conversion coatings on the electrical performance of LHE ZnNi

samples prepared using Dipsol materials and processes. Figure 1 compares cyclic potentiodynamic scans (CPDSs) for LHE ZnNi coatings on steel substrate tested in a 3.5% NaCl electrolyte. The CPDS results in Figure 1a indicated that bare ZnNi sample had approximately the same open circuit potential (OCP) of about -700mV on the forward and reverse scans. In contrast, the sample with a trivalent chromium conversion coating on top of the ZnNi coating had an OCP of about -750mV on the forward scan but about -650mV on the reverse scan. The increase in OCP of ~100 mV with the trivalent chromium passivation is an indication of the "self-healing" nature of the conversion coating and improved corrosion resistance.

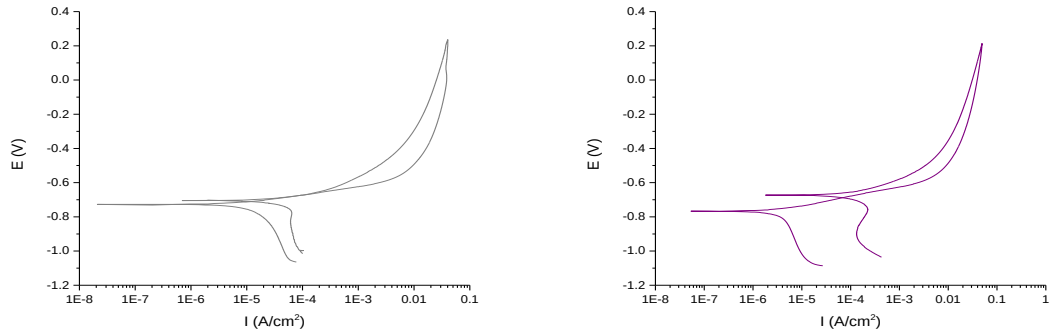

a b

Figure 1. CPDS of LHE ZnNi coatings on steel substrates that are: a) bare and b) coated with Dipsol IZ-264 trivalent chromium passivation

Electrochemical impedance spectroscopy (EIS) testing of bare ZnNi and ZnNi with an IZ-264 trivalent chromium passivation are shown in Figure 2a. The Nyquist plots of the bare and coated samples demonstrate that the sample with the non-chromate passivation had a much higher impedance intercept (~5,000 Ω) compared to the non-conversion coated sample (~1,500 Ω). The increase in impedance is an indication that the conversion coating passivated the ZnNi surface. A plot of Bode impedance and phase angle as a function frequency (Figure 2b) demonstrates that the impedance of the conversion coated ZnNi is higher at all measured frequencies compared to the bare ZnNi surface. The Bode phase angle data as a function of frequency shows evidence of two time constants for each type of coating. The response curve of the Bode phase angle graph are not the same for the samples, another indication the passivation layer significantly influences the electrochemical nature of the coating system.

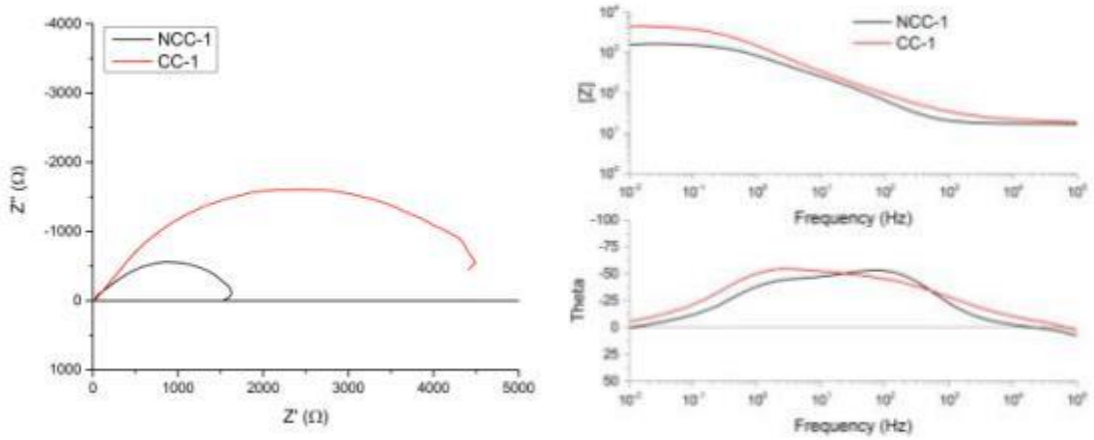

a b

Figure 2. Bare (NCC) and TCP conversion coated (CC) LHE ZnNi coatings on a steel substrate: a) Nyquist plot, b) Bode impedance and phase angle plots

Electrochemical corrosion testing of bare and coated LHE ZnNi samples was performed at +100mV compared to OCP in 3.5 wt% NaCl solution to remove ~ 1µm of the ZnNi coating. This process was intentional, with the intent to develop an accelerated procedure to provide insight into the response of the ZnNi coating to a corrosive environment. Corrosion current is shown as a function of time in Figure 3a for a bare ZnNi sample at a potential of +100mV to the OCP. The area under the curve corresponds to ~3A/cm^2-s, which is equivalent to the removal of ~1.1µm of the ZnNi coating. For reference, after about 20 minutes the measured corrosion current density was ~4mA/cm^2. Figure 3b shows the corresponding current density as a function of time graph of the LHE ZnNi with a non-chromate coating (Dipsol IZ-264) in which ~1 µm of coating (~2.8 A/cm^2-s) was etched away. The corrosion current density after 20 minutes was ~2.5 mA/cm^2 and the overall profile of the curve indicated a lower rate of corrosion. Scanning electron microscope (SEM) images of the bare Figure 4a and coated Figure 4b LHE ZnNi substrates are shown after accelerated corrosion testing. Focused ion beam (FIB) sectioning was done in the middle of the areas that were viewed to characterize the ZnNi coating. The images show that the surface of bare sample had significantly more texture and sharp features than the coated ZnNi substrate, an indication that the bare sample was susceptible to corrosive attack.

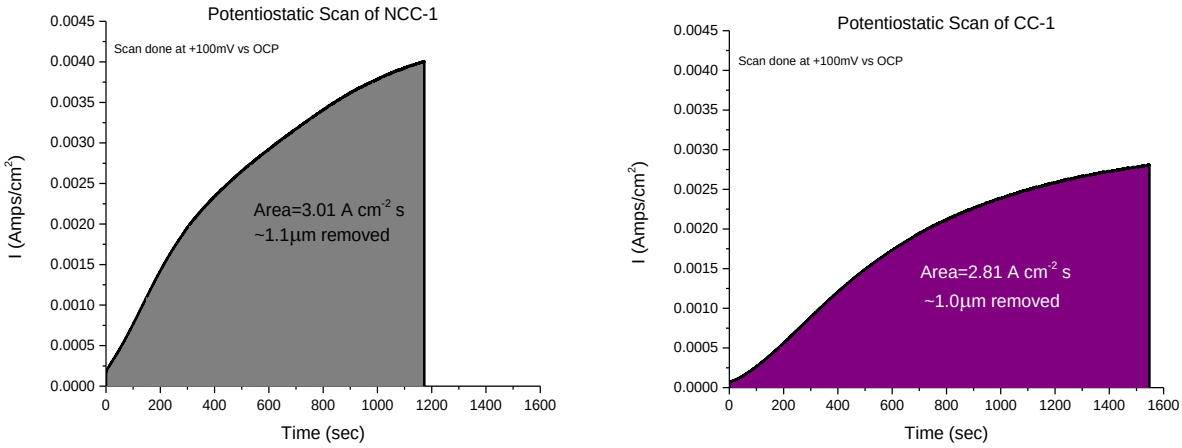

a b

Figure 3. Corrosion current density as a function of time for LHE ZnNi coatings on a steel substrate: a) bare and b) coated with Dipsol IZ-264 trivalent chromium passivation

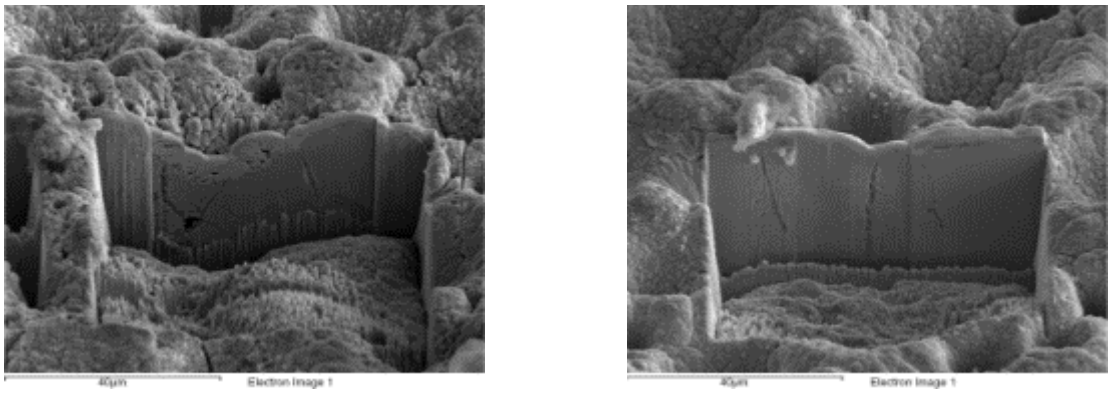

a b

Figure 4. SEM images of LHE ZnNI coatings on a steel substrate after FIB sectioning: a) no passivation; and b) with a Dipsol IZ-264 trivalent chromium passivation

Materials and Methods

Six different passivation coatings were evaluated. All coatings were deposited on electroplated with γ-ZnNi that had been deposited on steel substrates. The γ-ZnNi contained about 14 wt% nickel and was about 11 μm thick. A commercially available TCP coating (IZ-264), a cobalt-free TCP (Co-Free) and a modified cobalt-free TCP (Co-Free Mod); and a commercially available CrCC coating (IZ-258), were provided by Dipsol of America already deposited on the prepared substrates. Steel substrates electroplated with γ-ZnNi were also provided for the deposition of the CeCCs. Two types of CeCCs were produced; one being derived from chloride-based salts (CeCC-Cl) and the other from nitrate-based salts (CeCC-N).

Cerium-based Passivation Deposition

The γ-ZnNi substrates were first cleaned with ethanol. Then the substrates were alkaline cleaned in a 5 wt% Turco solution at 55˚C for 5 minutes to degrease the surface. A 1 ml/L HCl solution surface activation was used for 30 seconds at room temperature. Then the substrates went through either one of two deposition baths. One bath was based on a cerium chloride salt and the other a cerium nitrate salt. The cerium chloride salt bath consisted of 4.2 wt% cerium chloride hexahydrate (Alfa Aesar, 99.9%), 4.2 wt% (Fisher Scientific, 34-37% technical grade) hydrogen peroxide solution and 0.3 wt% (Rousselot DSF) gelatin in an aqueous solution. The cerium nitrate salt bath consisted of 4.8 wt% cerium nitrate heptahydrate (Acros Organics, 99.5%), 0 to 4.1 wt% (Fisher Scientific, 34-37% technical grade) hydrogen peroxide and 0.3 wt% (Rousselot DSF) gelatin in an aqueous solution. The substrates were immersed in either bath at a pH of 2 for up to 2 minutes at room temperature. A post-treatment of the cerium coatings were done in a 2.5 wt% sodium phosphate monobasic dihydrate (Fisher Scientific, 99.8%) solution at 85˚C for 5 minutes. The process used is shown in Figure 5.

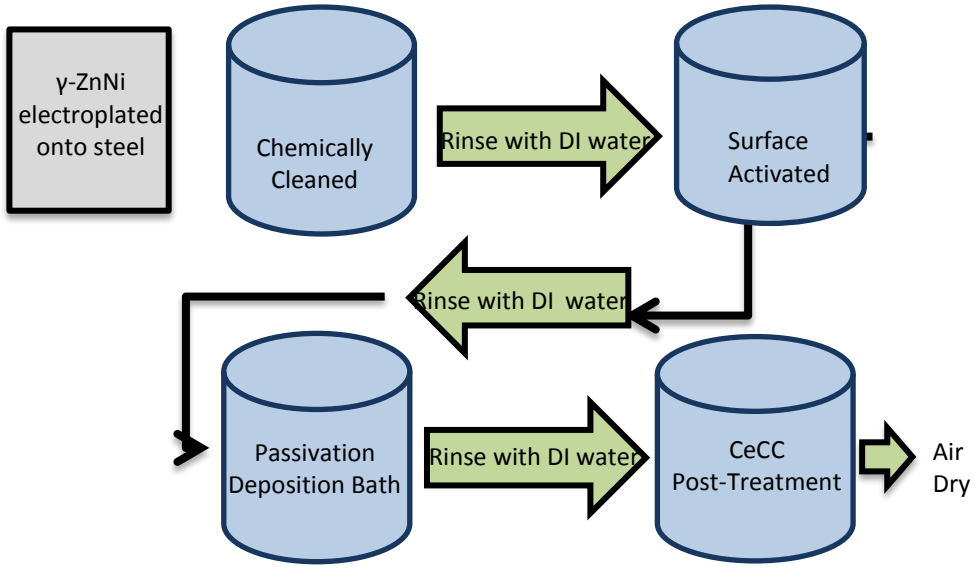

Figure 5. Process flow chart for deposition of cerium based passivations on LHE ZnNi

Trivalent and Hexavalent Chromium Based Passivation Deposition

The deposition of the TCP based passivations (standard TCP, Co-free TCP, and Co-free modified TCP) and hexavalent chromate passivation onto LHE ZnNi was done at Dipsol of America facilities in Livonia, MI. The process flow chart for those passivations is presented in Figure 6.

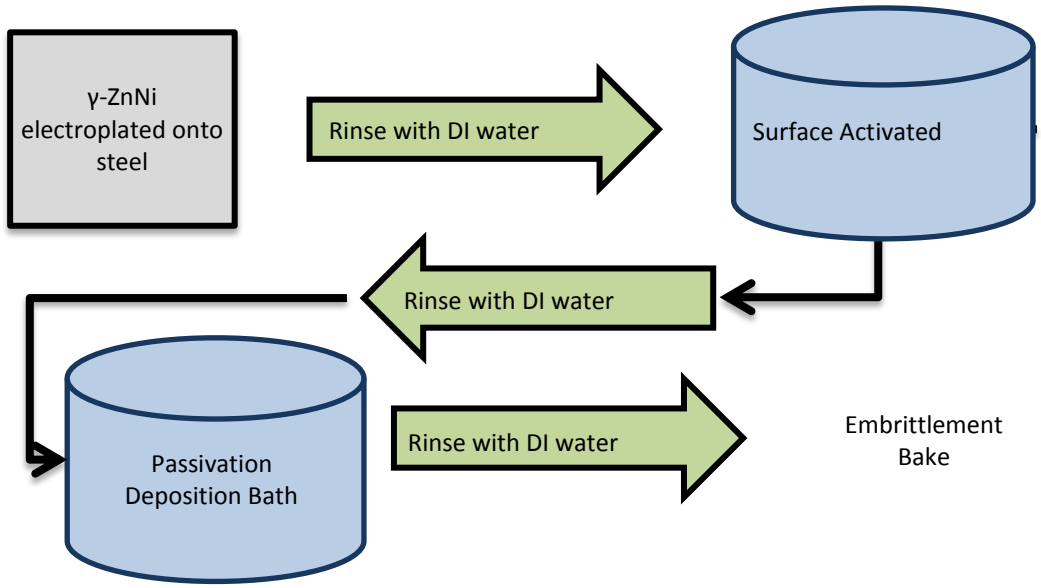

Figure 6. Process flow chart for depositions of trivalent and hexavalent chromium passivations on LHE ZnNi

Corrosion Resistance.

Corrosion resistance was evaluated in salt spray testing (Q-fog, Q-Panel Lab products) performed according to ASTM B117. A 5 wt% sodium chloride solution was used, as specified in the standard. The testing was performed on each of the coatings for 1000 hours. The coatings were visually evaluated at 100-hour intervals.

Electrochemical Analysis.

A flat cell (model K0235, Princeton Applied Research), with an SCE electrode, was used for all the electrochemical analysis. The electrolyte used was an aqueous solution containing 0.6 M ammonium sulfate and 0.6 M sodium chloride. Experiments were conducted using a potentiostat (EG&G Princeton Applied Research, Model 273A) and a frequency response analyzer (Solartron Instruments, SI 1255). The software used for data collection and analysis was from Scribner Associates, Inc. Zplot and Zview software packages were used for EIS data collection and analysis, respectively. Corrware and CorrView software packages were used for CPDS data collection and analysis, respectively. Reported results from electrochemical analyses were the average of four different measurements performed at different locations on each specimen.

Prior to analysis, the coatings were allowed to reach their open circuit potential (OCP) over a time period of 2000 seconds before starting electrochemical impedance spectroscopy (EIS). EIS was run over a frequency range of 10^{-2} to 10^{5} Hz with AC amplitude of 10 mV. After EIS, cyclic potentiodynamic scans (CPDS) were run at a 1.5 mV/s scan rate and ran from -0.4 V from OCP to OCP for the cathodic sweep and from OCP to -0.6 V from the OCP for the anodic sweep. The maximum overpotential reached during the scan was at 0.7 V from OCP.

Contact Resistance.

A device was built to test contact resistance as specified in MIL-DTL-81706. The device used two solid copper electrodes one of which was a 1 in^2 area that made contact with the coating covered side of the sample. The second electrode was slightly bigger and made contact with the exposed metal side of the sample. A pressure of 200 psi was applied to the electrode. A multi-meter measured the contact resistance in four-terminal resistance mode. Five measurements were taken from different areas on each panel to determine the reported values. A picture of the test apparatus is shown in Figure 7.

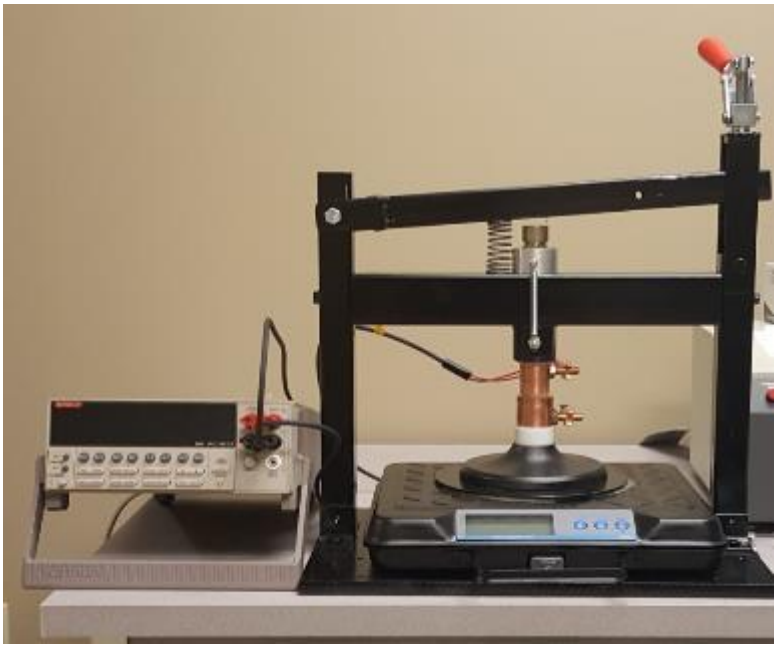

Figure 7. Electrical contact resistance testing set-up per MIL-STD-81706

Results and Discussion

Two sets of passivation layers on LHE γ-ZnNi were evaluated during the yearlong project. The first set of passivations were developed and evaluated during the first six months of the study to screen the most promising alternatives to hexavalent chromium and to establish procedures to evaluate the different samples. The second set of passivated ZnNi samples were fabricated using the most promising passivation materials and processing conditions in order to directly compare test results between types of passivations. Extensive characterization of the second set of samples was conducted to provide additional insight into the behavior and function of the passivation layers.

First Set of Passivation Samples

During the first half of the project baseline testing and evaluation of hexavalent chromium (CrCC), standard trivalent chromium passivation (TCP or Cr(III)), cobalt-free TCP (Co-Free), cerium nitrate based conversion coatings (CeCC-N) and cerium chloride based conversion coatings (CeCC-Cl) was completed.

As a part of the initial evaluation, optical and scanning electron images of the as-deposited LHE γ-ZnNi samples with and without passivations were taken. As shown in Figure 8 below optical images of uncoated and TCP coated ZnNi surfaces had a morphology that consisted of round features and particle sizes in the tens of micrometers range. The scanning electron image of an uncoated LHE ZnNi sample presented in Figure 9 depicts a typical as-deposited surface with rounded features and grain sizes on the order of ~10 to 20 µm. A profile plot of the surface of a LHE ZnNi sample is depicted in Figure 10 demonstrating that the distance between the peak and valley values was a few micrometers, an indication of the roughness of the electroplated coating.

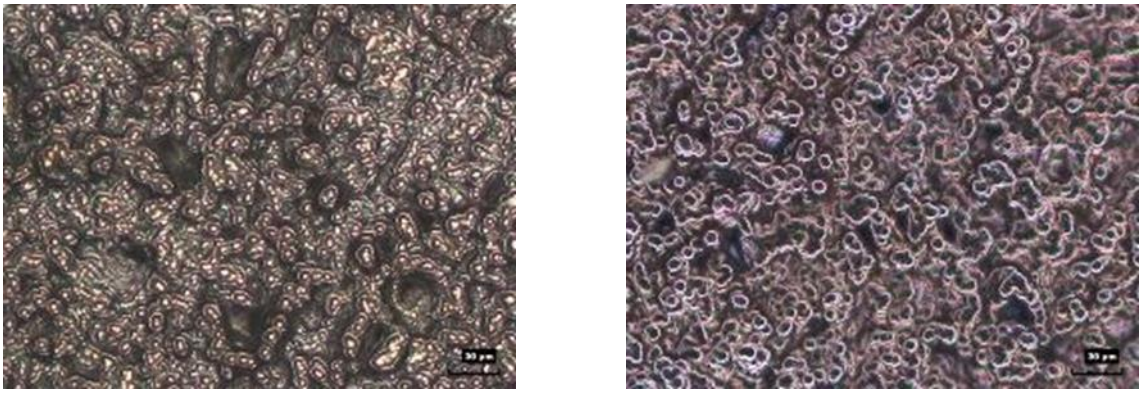

a b

Figure 8. Optical images of a) uncoated LHE ZnNi surface and b) TCP coated ZnNi surface

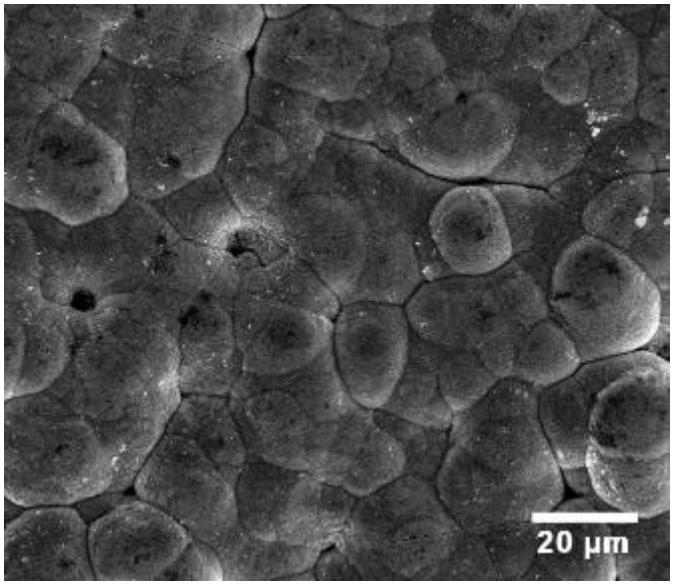

Figure 9. Scanning electron image of the top surface of uncoated electroplated LHE ZnNi

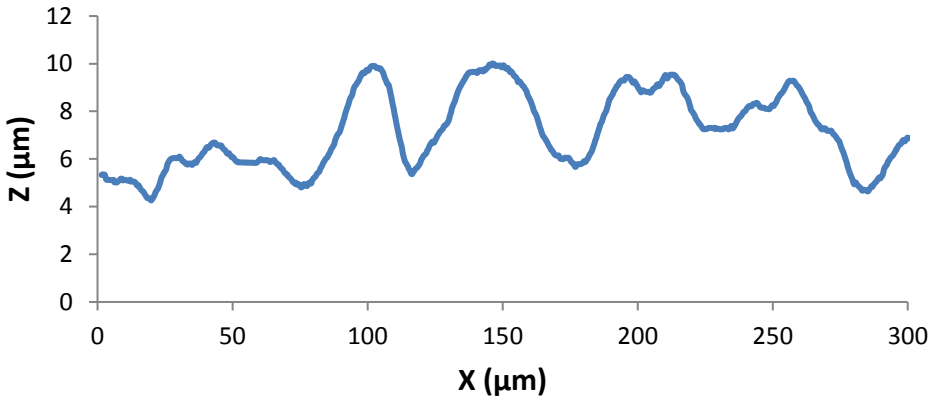

Figure 10. Topological profile plot across an uncoated, electroplated LHE ZnNi surface

A focused ion beam (FIB) scanning electron microscope was used to determine the thickness of passivation layers on LHE ZnNi. Shown in Figure 11 is a micrograph cross-sectional view of a TCP passivation on a ZnNi coating (the Pt is deposited in the FIB in order to preserve the top surface layers during ion milling). Distance measurements conducted in the FIB indicated that the TCP was ~100 nm thick. Similar results were found on this sample and for cerium coated samples.

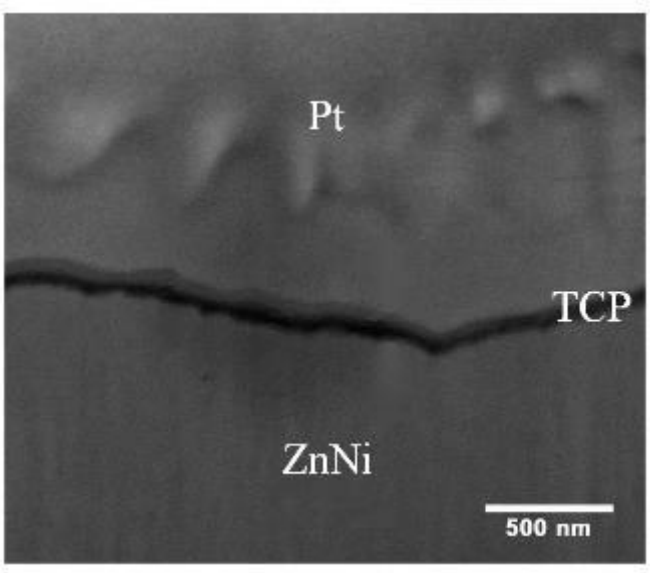

Figure 11. Cross-sectional image of a ~100 nm thick TCP layer on an electroplated ZnNi coating

Contact resistance measurements on the as-deposited samples were made on uncoated ZnNi, standard TCP (Cr(III)) passivated ZnNi, cobalt-free TCP, and several different versions of cerium nitrate and cerium chloride based passivations. Presented in Figure 12 are the results of the resistance testing that indicate the TCP and Co-free TCP had low resistance while the cerium based passivations had resistance values that were dependent on the deposition conditions but a few of the cerium based samples had values similar to the TCP based passivations.

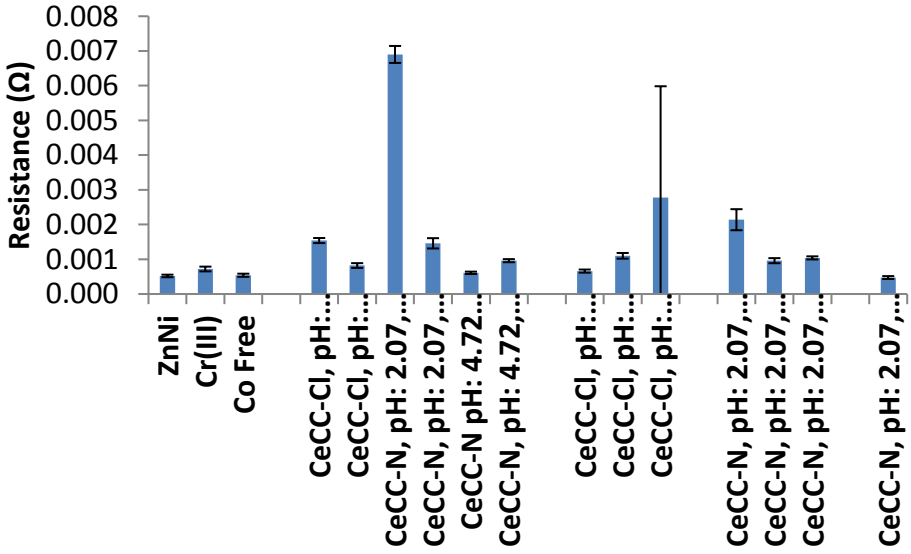

Figure 12. Contact resistance values of as-deposited LHE ZnNi samples with different passivations

The first group of samples were subjected to ASTM B117 salt spray exposure for up to 500 hours. Shown in Figure 13 are images of samples after salt spray for CrCC, TCP, Co-Free TCP, bare ZnNi and a number of different CeCC passivations (1-13). Visually the standard IZ-264 TCP performed the best with little to no corrosion visible. What is not apparent from the picture is that the corrosion product on the Co-Free TCP sample was thin with areas of non-uniform corrosion product. The contact resistance measurements of the samples after 500 hours are presented in Figure 14. The TCP passivations (standard and Co-Free) had the lowest values, the hexavalent chromium (CrCC) was very close to the maximum 10 mΩ specification value while the cerium based coating was well above the maximum value.

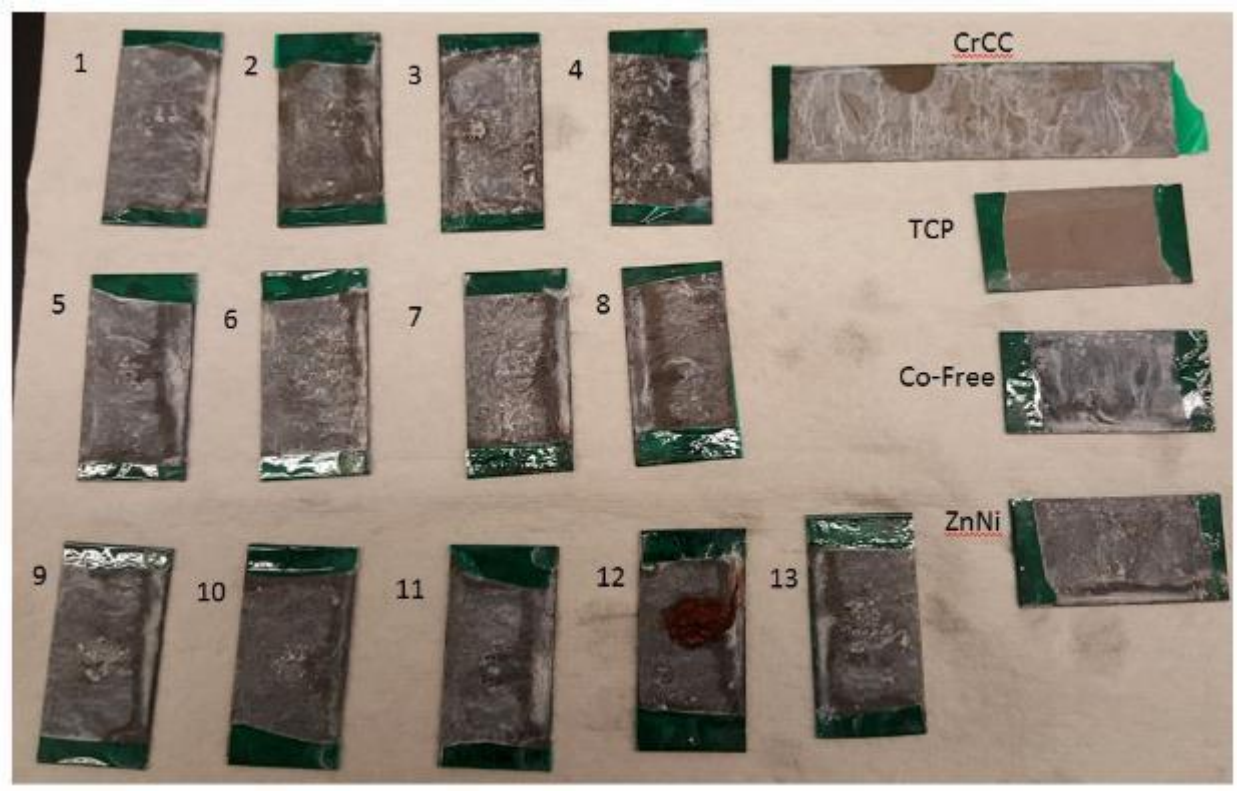

Figure 13. Images of LHE ZnNi samples with different passivation layers (CeCC are 1-13) after 500 hours of ASTM B117 salt spray exposure

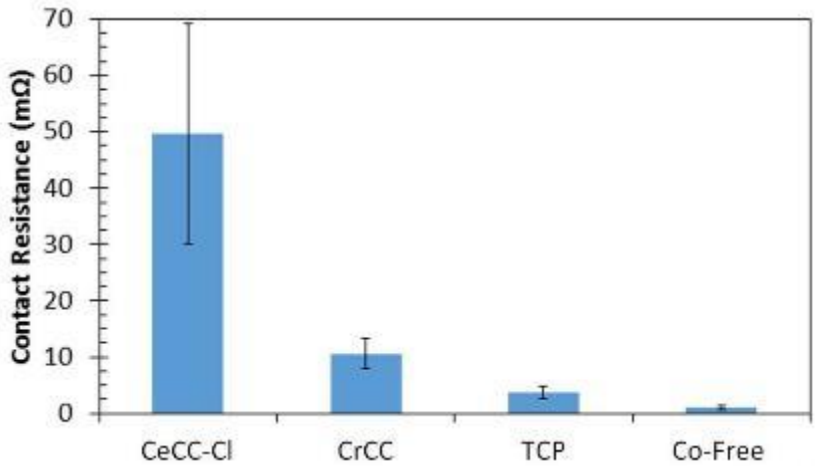

Figure 14. Contact resistance values of LHE ZnNi samples with different passivation layers after 500 hours of ASTM B117 salt spray exposure

The first set of samples were used to identify the most promising passivations based on deposition process, contact resistance, and performance during salt spray testing. Results indicated that the standard TCP, Co-Free TCP, and certain CeCC passivations on LHE ZnNi were able to meet the as-deposited contact resistance requirement of < 5 mΩ. Exposure to ASTM B117 salt spray conditions indicated that the TCP and Co-Free TCP had less visible corrosion and lower contact resistance than the hexavalent chromate passivation used as a reference.

Second Set of Passivation Samples

After evaluation of the first set of passivated LHE γ-ZnNi a second group of samples were prepared using deposition conditions that resulted in the best test results on the first set of samples. The second set of samples included hexavalent chromium (CrCC), standard trivalent chromium passivation (TCP or Cr(III)), cobalt-free TCP (Co-Free), a modified cobalt-free TCP (Co-Free Mod), a cerium nitrate based conversion coating (CeCC-N) and a cerium chloride based conversion coating (CeCC-Cl) passivation layers.

The as-deposited contact resistance of the six different passivation layers are presented in Figure 15. All of the contact resistance values were less than the specification of 5 mΩ except for the CeCC-Cl samples. The range in the measured values was a reflection of the average, with the greatest deviation for the CeCC-Cl samples.

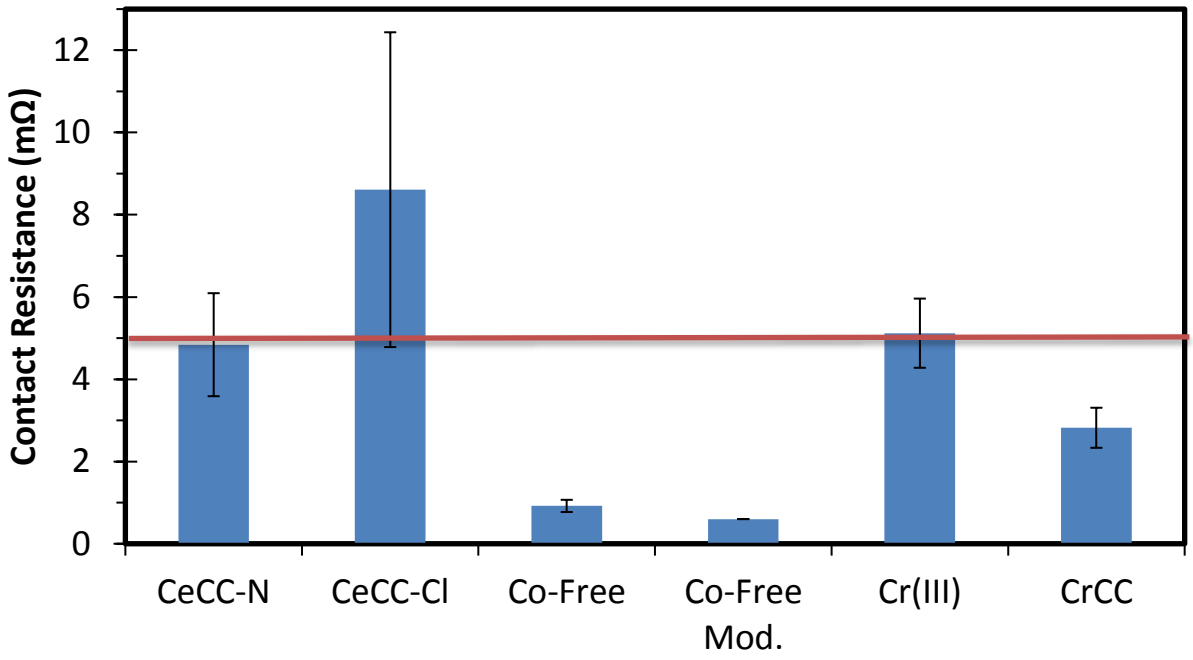

Figure 15. Contact resistance values of as-deposited LHE ZnNi samples with different passivation layers

Electrochemical impedance measurements were made on each of the as-deposited passivation layer samples. Presented in Figure 16 are the Bode plots of phase angle vs. frequency for all of the passivation layers evaluated. The differences in the curves in Figure 16 demonstrate that the 100 nm thick surface passivation layer can have a significant influence on the electrochemical response of the coating system.

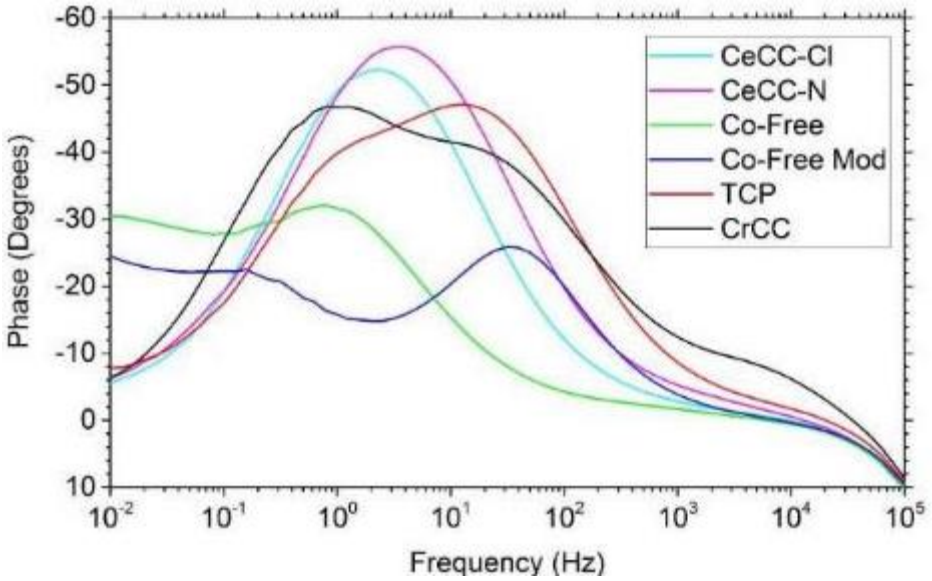

Figure 16. Bode phase angle plots for as-deposited passivation layers on LHE ZnNi

Within Figure 16 three subsets of samples have similar Bode plots. The CeCC passivated samples have a simple barrier response curve with a peak value between 50° and 60° at a frequency between 10^0 (1) and 10^1 (10) Hz (Figure 17). Standard TCP and CrCC passivations had double peak values at ~1 and ~10 Hz between phase angles of 40° and 50° (Figure 18) while the Co-Free and Co-Free Mod passivations had maximum phase angles between 20° and 30° at frequency values of ~1 Hz (Co-Free) and ~50 Hz (Co-Free Mod) as shown in Figure 19. The two time constants (double peaks) in Figures 18 and 19 most likely indicate that the TCP-based and CrCC passivations have both an active and passive (barrier) protection mechanism while the Ce-based passivation are just a barrier (single time constant or one peak).

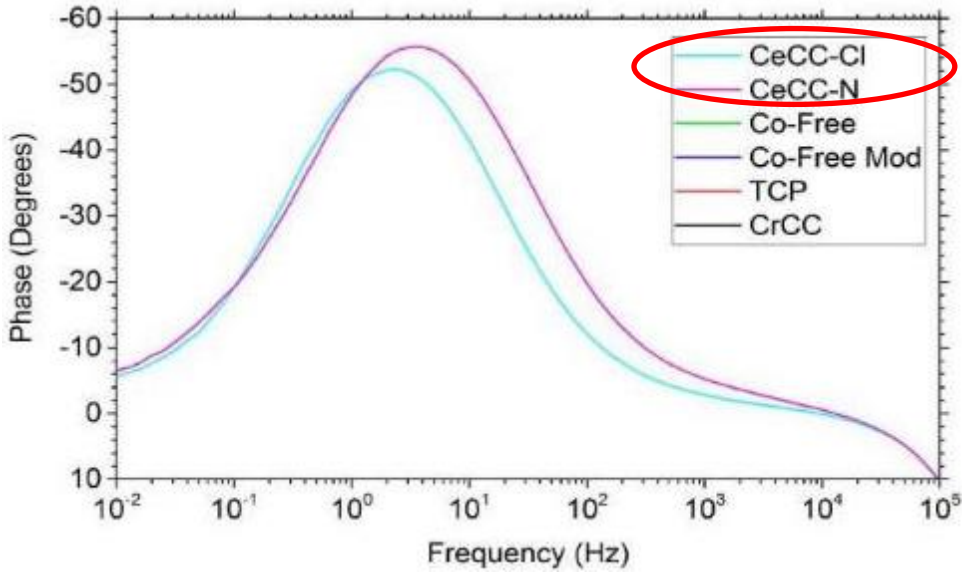

Figure 17. Bode phase angle plots for CeCC passivation layers on LHE ZnNi

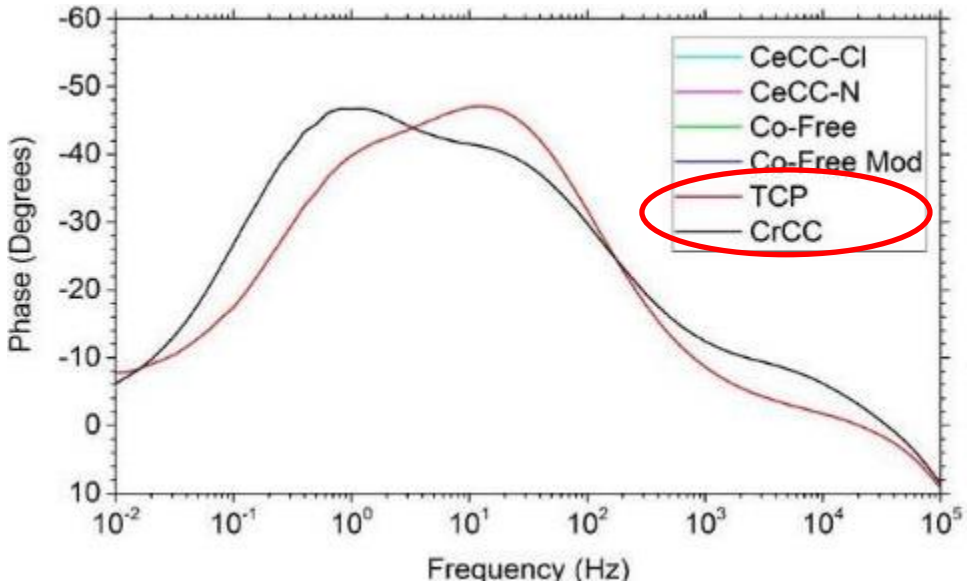

Figure 18. Bode phase angle plots for TCP and CrCC passivation layers on LHE ZnNi

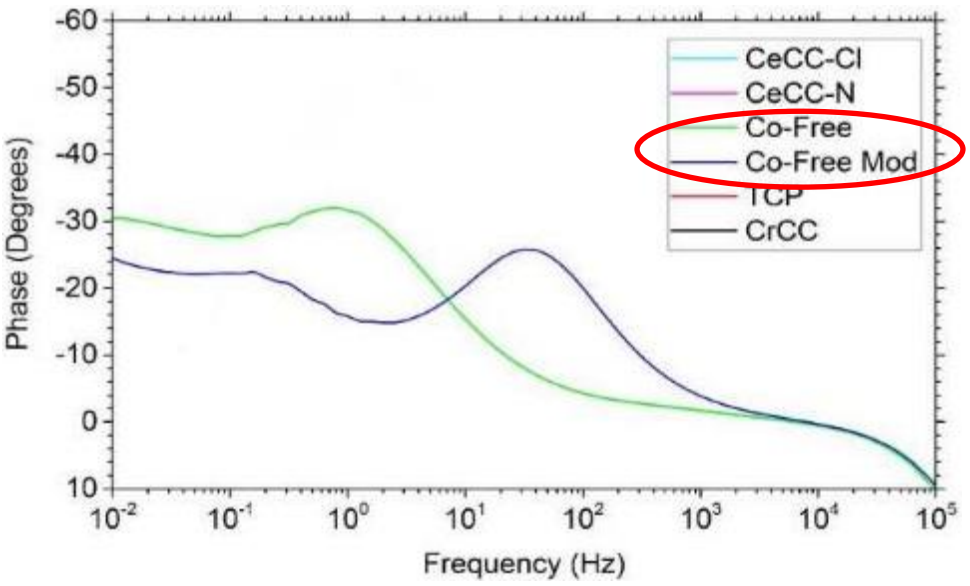

Figure 19. Bode phase angle plots for Co-Free and Co-Free Mod passivation layers on LHE ZnNi

Electrochemical polarization tests performed on the as-deposited passivation layers indicated that the open circuit potential of the samples was between -1.1 and -0.9V depending on the type of passivation used (Figure 20). This result is consistent with the Bode phase angle plots in that the surface layer passivation influenced the electrochemical properties of the coating system. After the passivation layer begins to break down and the peak corrosion current of ~$5x10^{-1}$ A/cm^2 occurs at a potential of ~ -0.1V all of the samples had a corrosion potential very close to the value of -0.673V associated with oxidation of Zn in water. Collectively the polarization data indicate that initially the passivation layer dominates the electrochemical/corrosion behavior of the samples but once the passivation layer breaks down that oxidation of zinc occurs.

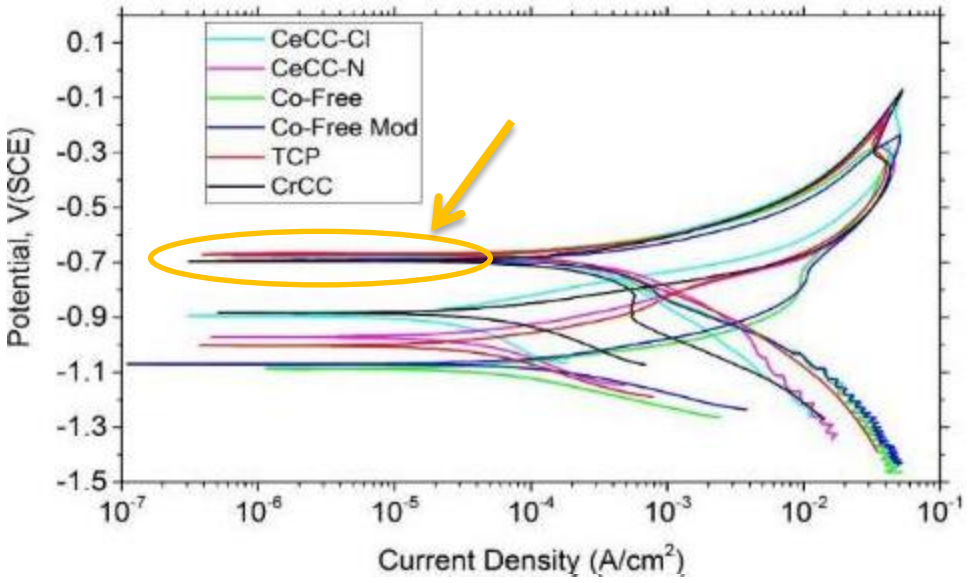

Figure 20. Polarization curves for all six as-deposited passivation layers

Exposure of the second set of passivated samples to ASTM B117 neutral salt spray for 1000 hours was done. Observation and electrical contract resistance testing of the samples after 100 hours were conducted to provide data on the initial response of the coating system to salt spray conditions. After 1000 hours of B117 the cerium passivated samples had heavy salting (Figure 21). The CrCC sample had visible corrosion product across the surface while the standard IZ-264 TCP sample did not have any macroscopically visible corrosion product (Figure 22). While the Co-Free sample had some areas of heavy salting and other areas with light areas of corrosion (Figure 23), the Co-Free Mod sample had a very thin layer of corrosion product across the surface that appears to be more prominent in the image in Figure 23 than sample appeared to the eye. Visually the TCP and Co-Free Mod samples looked the best after 1000 hours of salt spray testing.

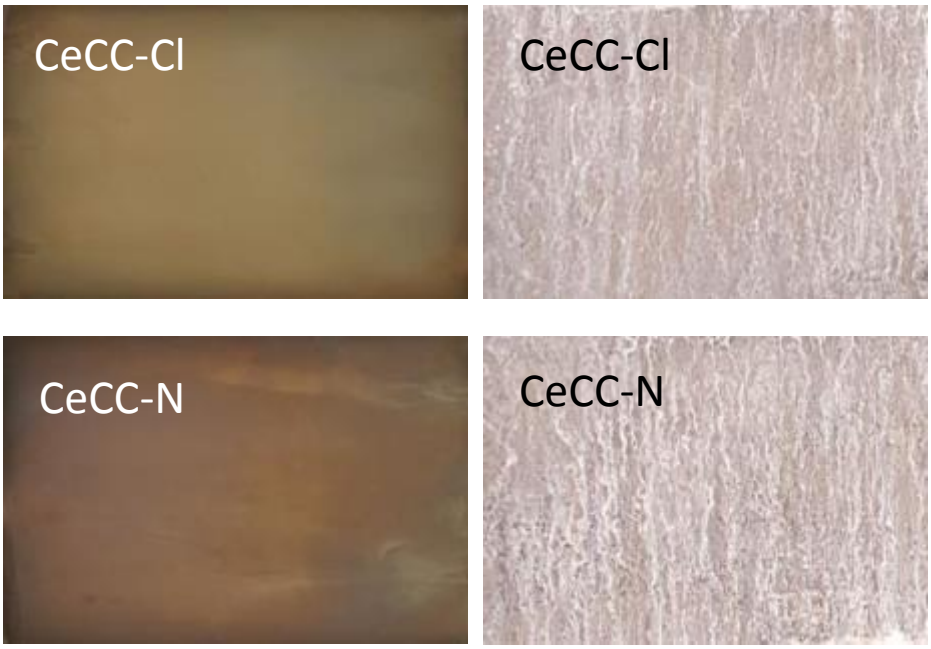

Figure 21. Optical images of CeCC passivated ZnNi samples before (left) and after (right) 1000 hours of ASTM B117 neutral salt spray exposure

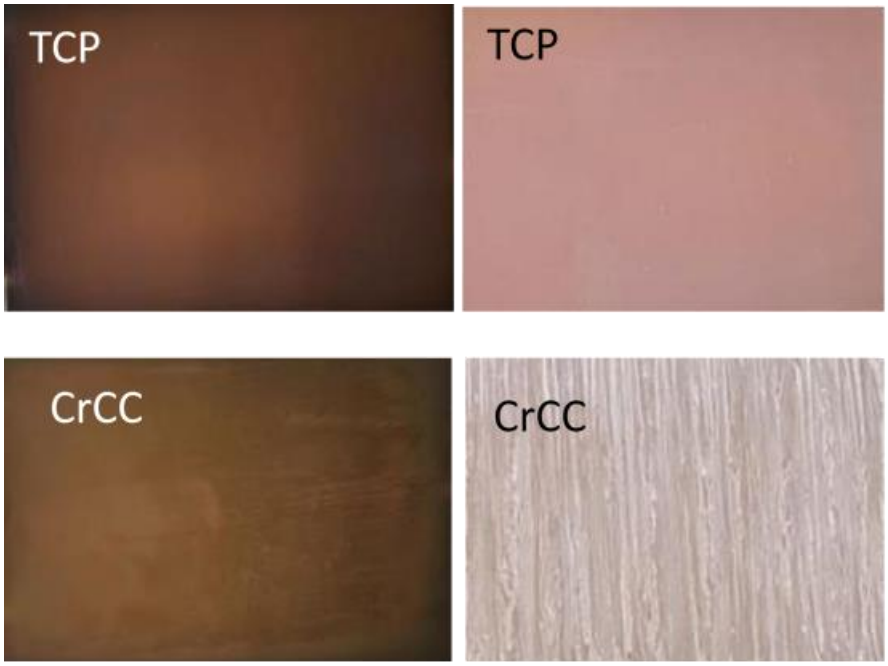

Figure 22. Optical images of standard IZ-264 TCP and CrCC passivated ZnNi samples before (left) and after (right) 1000 hours of ASTM B117 neutral salt spray exposure

Figure 23. Optical images of Co-Free TCP and Co-Free Mod passivated ZnNi samples before (left) and after (right) 1000 hours of ASTM B117 neutral salt spray exposure

Scanning electron images of the surface of the samples after 1000 hours of ASTM B117 exposures were taken to observe the morphology of the corrosion products. Shown in Figure 24 are the images from the CeCC samples that had extensive corrosion product on the surface but note that the morphology of the corrosion product is very different for the film deposited from the chloride solution than the one from the nitrate solution.

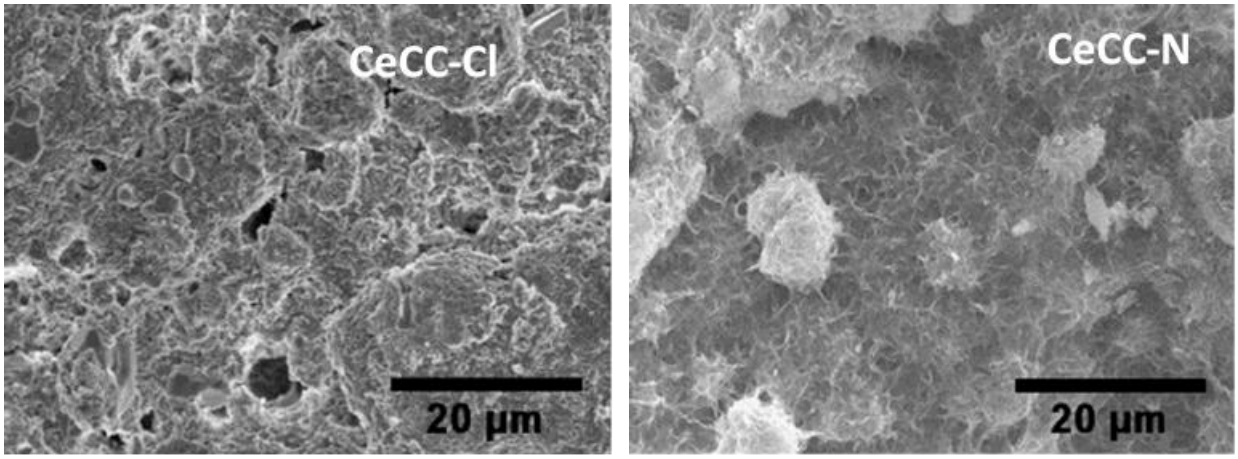

Figure 24. Scanning electron microscope images from the surface of CeCC passivated ZnNi samples after 1000 hours of ASTM B117 neutral salt spray exposure

The standard TCP passivation morphology had the rounded morphology of the as-deposited electroplated ZnNi (similar to that in Figure 9) while the CrCC samples had a featureless corrosion product that uniformly covered the entire surface (Figure 25). Morphologically the Co-Free and Co-Free Mod were very different, with the Co-Free sample having a layered corrosion product while the Co-Free Mod appeared to have localized (pitting) corrosion product on an otherwise corrosion free ZnNi surface.

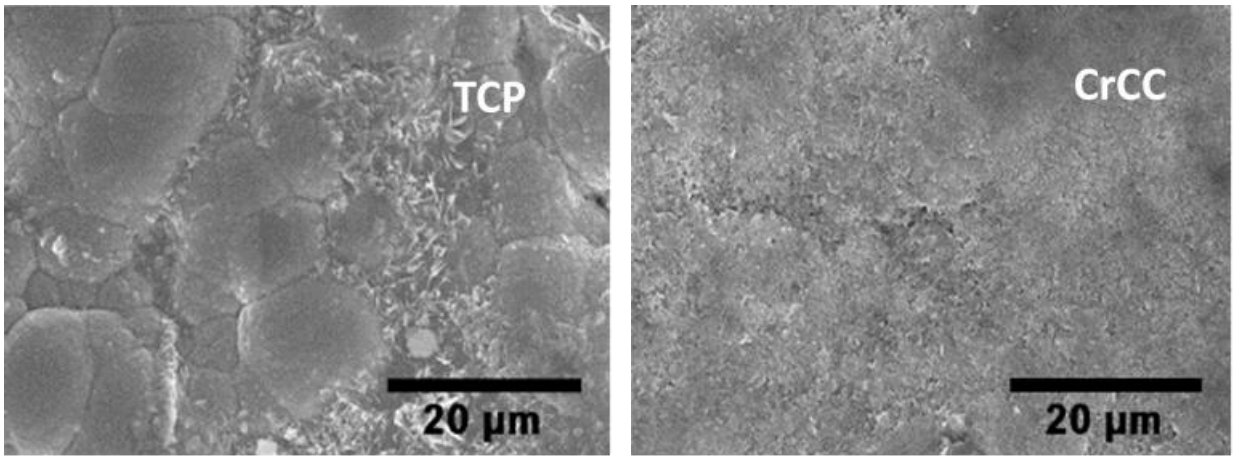

Figure 25. Scanning electron microscope images from the surface of standard TCP and CrCC passivated ZnNi samples after 1000 hours of ASTM B117 neutral salt spray exposure

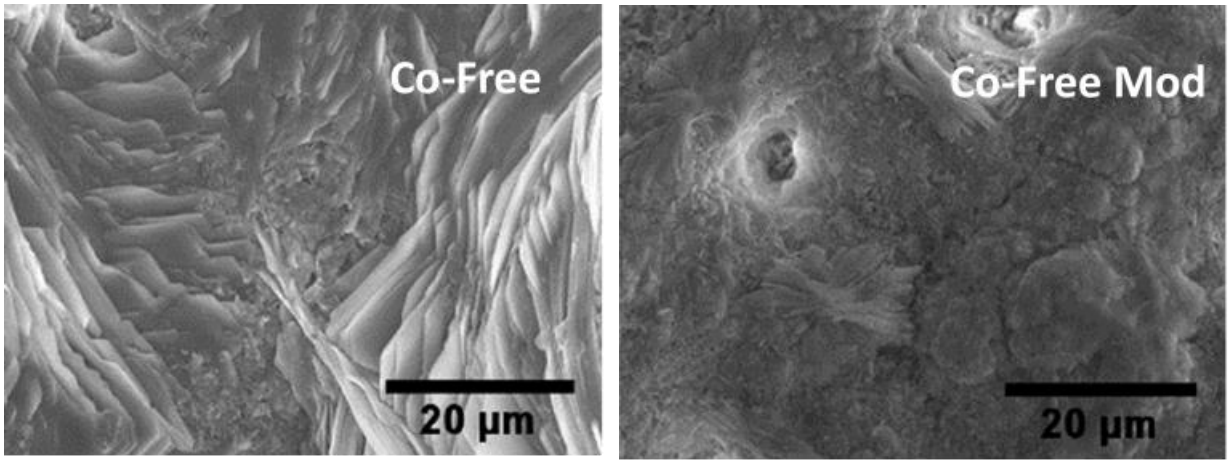

Figure 26. Scanning electron microscope images from the surface of standard Co-Free and Co-Free Mod passivated ZnNi samples after 1000 hours of ASTM B117 neutral salt spray exposure

After salt spray testing the maximum allowable contact resistance value is 10 mΩ/in^2. Depicted in Figure 27 are electrical contact resistance data from the initial (as-deposited), after 100 hours, and after 1000 hours of ASTM B117 exposure samples. (Data for TCP and CrCC after 100 hours were not taken due to a lack of samples.) The contact resistance values for both of the cerium passivations and the Co-Free sample were orders of magnitude above the threshold after 100 and 1000 hours. The CrCC measured contact resistance was >10^4 mΩ after 1000 hours. Consistent with the macroscopic observation of little to no visible corrosion product on the surface after 1000 hours of salt spray exposure, the Co-Free Mod and standard TCP had the lowest electrical contact resistance values measured of 8 mΩ/in^2 and 14 mΩ/in^2 respectively.

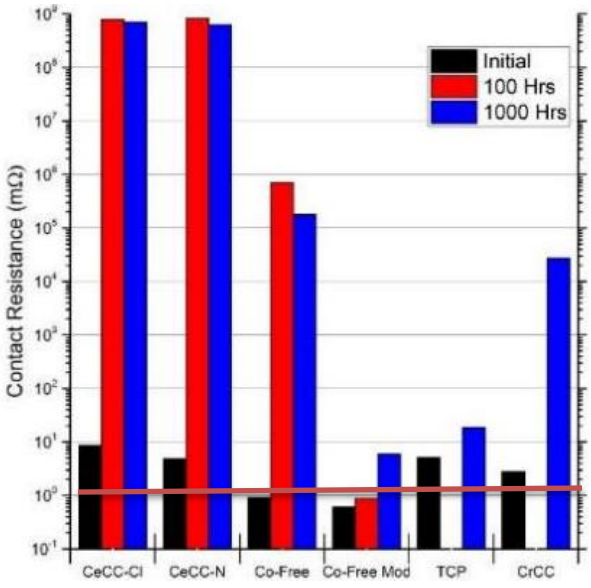

Figure 27. Electrical contact resistance values for the six passivation layers prior to and after ASTM B117 salt spray exposure

Characterization of the samples after salt spray testing using x-ray diffraction indicated that the corrosion product diffraction peaks on the surface of the cerium and Co-Free TCP between 10° and 35° of two theta was consistent with zinc oxide/hydroxide/carbonate structures (Figure 28). A small amount of corrosion product was detected on the CrCC sample but the peaks associated with zinc oxide/hydroxide/carbonate on the standard TCP and Co-Free Modified TCP were insignificant. The diffraction data was consistent with visual observations and electrical contact resistance data in that the TCP and Co-Free Mod TCP performed the best during salt spray exposure.

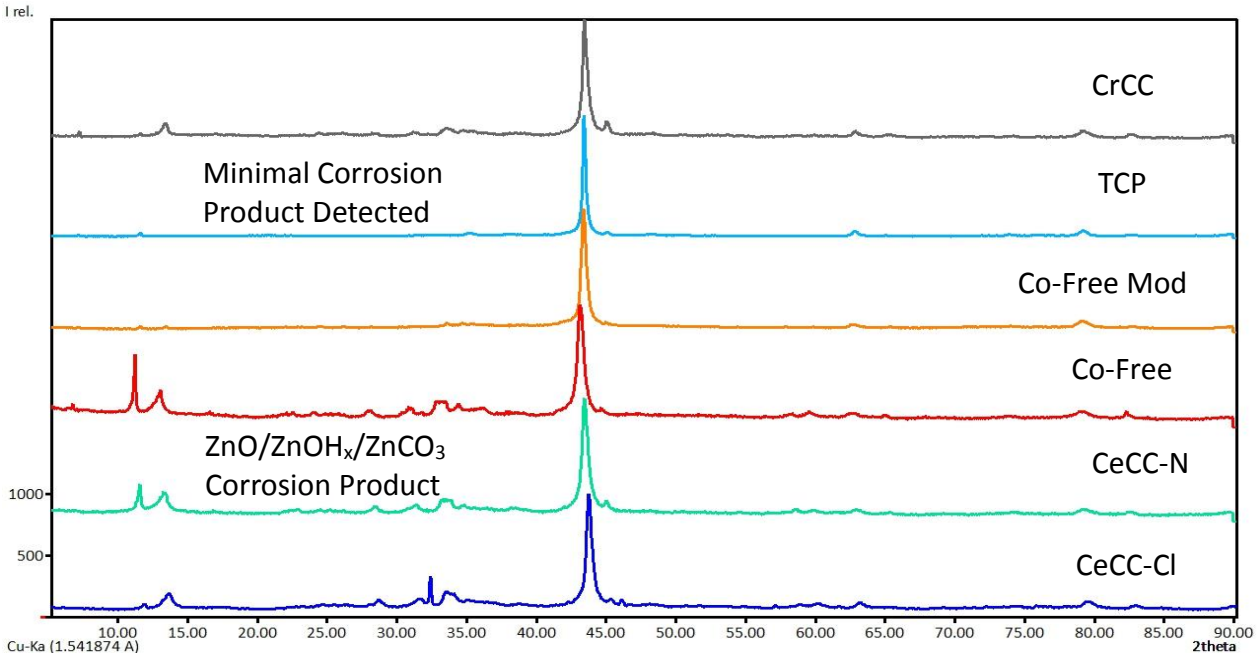

Figure 28. X-ray diffraction patterns for the six passivation layers after 1000 hours of ASTM B117 salt spray exposure

Electrochemical impedance testing of the samples after 1000 hours of salt spray exposure indicated that all of the samples demonstrated a simple barrier film response on the Bode phase angle plot (Figure 29). However, the two best performing passivation layers, TCP and Co-Free Mod, had peak phase angle values near 10 Hz while the other passivation layers had peak phase angle values below 1 Hz. The physical meaning of the difference in phase angle position is likely related to the lack of corrosion product on the TCP and Co-Free Mod surfaces.

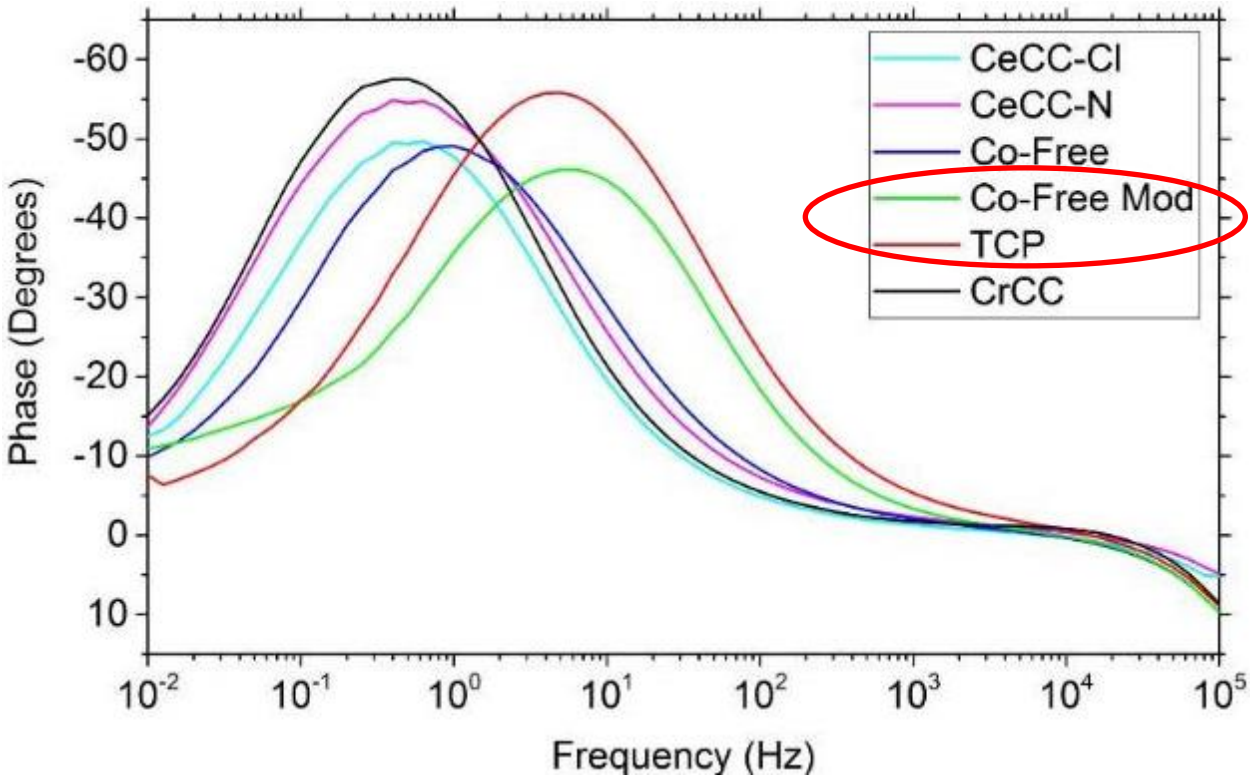

Figure 29. Bode phase angle plots for different passivation layers on LHE ZnNi after 1000 hours of ASTM B117 salt spray exposure

Alternative Contact Resistance Methodology

Currently the methodology specified in MIL-DTL-81706B is used to measure contact resistance in applications complying with MIL-DTL-38999L. While simple to setup and use, this methodology has low repeatability and is generally destructive to both the samples and the test setup. It also does not have the ability to map contact resistance on the substrate to facilitate quality control of coatings and processes. Development of an alternative methodology that is simple, repeatable, non-destructive, and capable of scanning across the substrate to produce a resistance map would be advantageous. During the project an alternative method based on a four line microprobe method for thin films was evaluated.

Four Line Microprobe Method

Researchers at Brigham Young University (BYU) describe, in a series of papers, a mathematical model and fabrication of a four line microprobe to measure contact resistance of thin film battery electrodes. [17,18] This probe is similar to the familiar four-point probe technique of measuring resistance. However, rather than conical tips for probes, four 10µm wide lines of 2-3mm length are used for the probes, as shown below in Figure 30.

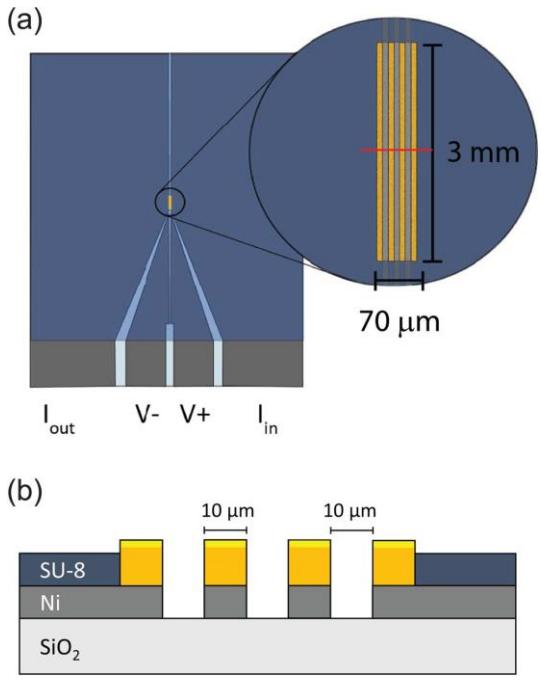

Figure 30. Four line microprobe geometry

In the original application, this probe is used in two electrical measurement configurations: 1. Tangential mode—which is essentially a normal 4 terminal measurement; and 2. Orthogonal mode—drives current from the two outer lines through the sample to the bottom of the sample and measures the resulting voltages on the inner lines. These configurations are shown in Figure 31.

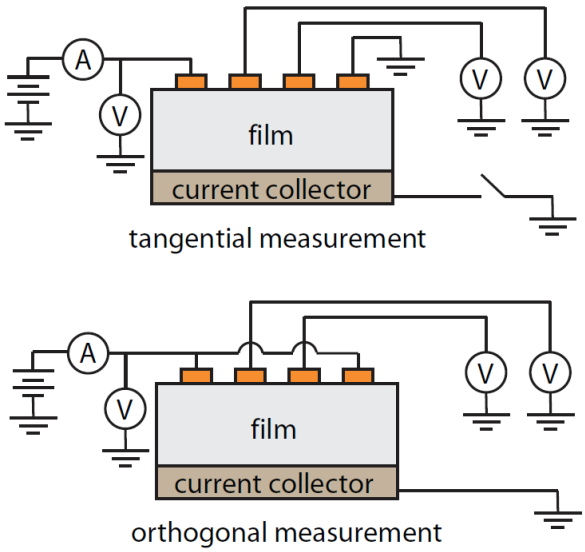

Figure 291. Tangential and Orthogonal measurement configuration

This methodology was verified using standard van der Pauw and four point probe methodologies by the research group at BYU.

Use of the Probe for Electrical Contact Resistance

A microprobe fabricated by BYU was purchased for evaluation. Since the publication of the papers, BYU had changed the design somewhat to a 6-line configuration (papers pending). However, this did not affect the evaluation; the two extra lines were ignored and it was used in a 4-line configuration. The probe was set up in a simple 4-terminal measurement configuration using a Keithley 2002 multimeter in 4-terminal resistance mode. Before measuring the integrity of the probe lines were verified using a HiROX digital microscope.

Per BYU instruction, initially ~10-15 lbs of force were used in making contact to a ZnNi sample using the probe. Despite multiple efforts, this amount of force was insufficient to make electrical contact. At this point we decided to use the MIL-DTL-81706B apparatus to make electrical contact to the probe. Because of insufficient headspace, no sample could be put in the apparatus when the probe was inserted. Therefore, the electrical resistance measurements were of the top copper electrode of the MIL-DTL-81706B apparatus. At a pressure of 60 psi, electrical contact was made to the probe and five measurements were taken: 0.0006 Ω, 0.0008 Ω, 0.0007 Ω, 0.0008 Ω, and 0.0008 Ω; giving a mean of 0.00074 Ω and a standard deviation of 0.0000894 Ω. At this point no more measurements could be taken; the probe had degraded beyond usability from moving it in the apparatus as shown in Figure 32 and Figure 33 the probes were damaged during testing.

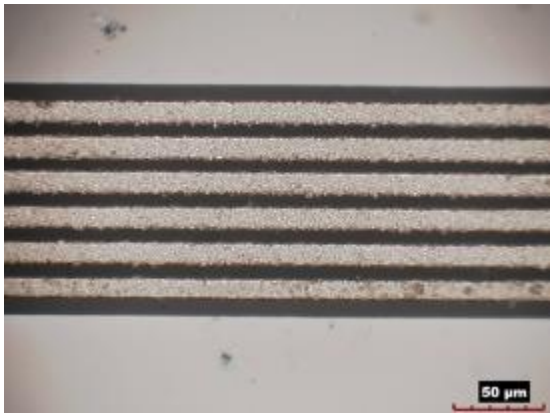

Figure 302. Probe lines before use

Figure 313. Probe lines after use

After ordering another probe from BYU, it was determined that the design rules had been changed: 20 µm lines rather than 10 µm and the lines would be 3 µm above the insulator rather than 1 µm. The MIL-DTL-81706B apparatus was modified to get more headspace to fit samples and allow good contact at 20 lbs of force. Samples that were coated with standard IZ-264 TCP, Co-Free TCP, and hexavalent chromium IZ-258 coatings were then measured using the new probe and modified testing apparatus. Results are summarized in Table I and indicate that the test methodologies give different values for measured resistance. A statistical T-test comparison of the mean values for the BYU and MIL-DTL resistance data indicated that there was a measurable difference between

the two methods for the IZ-264 and IZ-258 samples (>99% chance) but the Co-Free sample did not show a strong difference in the mean values (~22% chance). However, the BYU probe was not operated in the orthogonal mode which would have most closely approximated the MIL-DTL-81706B methodology.

Table 1. Comparison of BYU probe and MIL-DTL-81706B results

Sample	BYU Probe Resistance (ohms)	MIL-DTL-81706B Probe Resistance (ohms)	T-test comparison
IZ-C17 + IZ-264	0.0007 ± 0.0002	0.013 ± 0.001	>99% chance different
Co-Free	0.0013 ± 0.0005	0.00142 ± 0.00007	~22% chance different
IZ-C17 + IZ-258	0.0007 ± 0.0004	0.0062 ± 0.0009	>99% chance different

Conclusions and Implications for Future Research

Six different passivation layers on ZnNi for electrical connector applications was investigated using flat sheet samples. Hexavalent chromate passivation was used as a reference standard for the experimental IZ-264 trivalent chromium (TCP), Co-Free TCP, Co-Free Modified TCP, cerium chloride based and cerium nitrate based passivations that were developed. Based on the data generated and analysis conducted during the project the following can be concluded.

- As deposited trivalent chromium and cerium based passivations on electroplated LHE γ-ZnNi can have electrical contact resistance < 5 $m\Omega/in^2$ specification using optimized deposition conditions.
- The electrochemical response of the as deposited passivation layers is dependent on the type of material and process used. Cerium based passivations have a single time constant response that implies a simple barrier response. The TCP and CrCC passivations have two time constants that infer an active electrochemical response in addition to being a physical barrier.
- After 1000 hours of exposure to ASTM B117 salt spray conditions the standard IZ-264 TCP and Co-Free Modified TCP samples had electrical contact resistance values less than the 10 $m\Omega/in^2$ upper limit specification. All of the other passivations investigated were well above the maximum contact resistance value.
- An alternative contact resistance test method based on a four line microprobe method was investigated. The results indicated that the microprobe method may be a more sensitive and reproducible test approach than MIL-DTL-81706B.

With respect to the future research, additional evaluation of the standard IZ-264 TCP and Co-Free Modified TCP coatings on shaped and formed electrical connectors should be conducted to determine if the systems can meet military requirements such as MIL-DTL-38999. The development of a more sensitive and reproducible contact resistance method would enable faster development of alternative passivations and provide improved quality control process tests for existing passivations.

Literature Citations

1. H. L. J. Archer, W. J. Powell and J. T. Menke, "Method for Deposition of Steel Protective Coating". United States Patent 7514153, 7 April 2009.

2. "EPA Technology Transfer Network Air Toxics Website Cadmium Compounds," Enivronmental Protection Agency, 18 October 2013. [Online]. Available: http://www.epa.gov/airtoxics/hlthef/cadmium.html#ref1. [Accessed 26 February 2014].

3. M. G. Hosseini, H. Ghiasvand and H. Ashassi-Sorkhabi, "Preparation Ce(III) conversion coatings on electrodeposited Zn-Ni alloy and comparison of their corrosion performance and morphology with Cr(VI) conversion coatings," *Surface Engineering*, vol. 29, no. 1-5, 2013.

4. M. Ferreira, R. G. Duarte, M. F. Montemor and A. Simoes, "Silanes and rare earth salts as chromate replacers for pre-treatments on galvanised steel," *Electrochimica Acta,* vol. 49, pp. 2927-2935, 2004.

5. M. H. Sohi and M. Jalali, "Study of the corrosion properties of zinc–nickel alloy electrodeposits before and after chromating," *Journal of Materials Processing Technology,* vol. 138, pp. 63-66, 2003.

6. "EPA Technology Transfer Network Chromium Compounds," Environmental Protection Agency, 18 October 2013. [Online]. Available: http://www.epa.gov/ttnatw01/hlthef/chromium.html. [Accessed 26 February 2014].

7. F. Blin, P. Koutsoukos, P. Klepetsianis and M. Forsyth, "The corrosion inhibition mechanism of new rare earth cinnamate compounds—Electrochemical studies," *Electrochimica Acta,* vol. 52, pp. 6212-6220, 2007.

8. F. Blin, S. G. Leary, G. B. Deacon, P. C. Junk and M. Forsyth, "The nature of the surface film on steel treated with cerium and lanthanum cinnamate based corrosion inhibitors," *Corrosion Science,* vol. 48, pp. 404-419, 2006.

9. L. Zeng, C. J. Brown, M. W. Smith, L. Haylock, R. H. Gurrola, E. Monserratt, and D. Youngblood, “Evaluation of Alternatives to Electrodeposited Cadmium for Threaded Fastener Applications”, SAE International Technical Paper 2006-01-3169, 2006.

10. R. Misiaszek, “Alternatives to Cadmium Plated Military Connectors and Fasteners”, Aerospace/Defense Industry Supply Chain Conference: Chemicals of Concern and Safer Solutions, Sturbridges, MA, September 24, 2013.

11. S. P. Sitaram, J. O. Stoffer, and T. J. O'Keefe, "Application of conducting polymers in corrosion protection", *J. of Coatings Tech*, vol. 69 (866), pp 65-69, 1997.

12. J. O. Stoffer, T. J. O'Keefe, M. O'Keefe, E. Morris, S. Hayes, P. Yu, and X. Lin, "Environmentally safe aircraft conversion coatings", International SAMPE Technical Conference, vol. 32, pp 879-888, 2000.

13. M. O'Keefe, B. Fahrenholtz, E. Morris, and R. Albers, "Corrosion resistant polymer coatings containing rare earth compounds", National Association for Surface Finishing Annual Conference SUR/FIN 2013, pp. 501-513, 2013.

14. M. O'Keefe, W. Fahrenholtz, and B. Curatolo, "Multifunctional UV (MUV) curable corrosion coatings for aerospace applications", Metal Finishing, pp. 28-31, February 2010.

15. M. J. O'Keefe, W. G. Fahrenholtz, J. O. Stoffer, and E. L. Morris, "Corrosion Resistant Polymer Coatings Containing Rare Earth Compounds", in Rare Earth Based Corrosion Inhibitors, M. Forsyth and B. Hinton ed., Woodhead Publishing, (in press, 2014).

16. S. Maddela, C. Castano, M. O'Keefe, Y.-M. Wang, T. Lingenfelter, and S. Cheng, "Corrosion Protection of Mg-Al-Galvanized Steel Assemblies", 9th International Conference on Magnesium, Vancouver, BC, Canada, July 2012.

17. J. D. Flygare, A. A. Riet, B. A. Mazzeo, D. R. Wheeler, "Mathematical Model of Four-Line Probe to Determine Conductive Properties of Thin Film Battery Electrodes", *J. of Electrochem. Soc.*, vol. 162 (10), pp A2136-A2144, 2015.

18. B. J. Lanterman, A. A. Riet, N. S. Gates, J. D. Flygare, A. D. Cutler, J. E. Vogel, D. R. Wheeler, B. A. Mazzeo, "Micro-Four-Line Probe to Measure Electronic Conductivity and Contact Resistance of Thin-Film Battery Electrodes", *J. of Electrochem. Soc.*, vol. 162 (10), pp A2145-A2151, 2015.

Appendices

Supporting Data

List of Scientific/Technical Publications

Articles in Peer-reviewed Journals

Technical Reports

Conference or Symposium Scientifically Recognized

S. Volz, J. Claypool, M. O'Keefe, and W. Fahrenholtz, "Materials Characterization of Electroplated –ZnNi with Passivation Layers", Materials Science & Technology Conference 2016, Oct 24-27, 2016, Salt Lake City, UT.

S. Volz, J. Claypool, M. O'Keefe and W. Fahrenholtz, "Corrosion Behavior and Contact Resistance of Electroplated γ–ZnNi with Passivation Layers", 229th Electrochemical Society Meeting, May 29-June 2, 2016, San Diego, CA.

Conference or Symposium Abstracts

Text Books or Chapters

Other Supporting Materials